We are IntechOpen, the world's leading publisher of Open Access books Built by scientists, for scientists

4,800
Open access books available

122,000
International authors and editors

135M
Downloads

Our authors are among the

154
Countries delivered to

TOP 1%
most cited scientists

12.2%
Contributors from top 500 universities

WEB OF SCIENCE™

Selection of our books indexed in the Book Citation Index in Web of Science™ Core Collection (BKCI)

Interested in publishing with us?
Contact book.department@intechopen.com

Numbers displayed above are based on latest data collected.
For more information visit www.intechopen.com

3

Some Methods for Improving the Reliability of Optical Porous Silicon Sensors

Tanya Hutter[1] and Shlomo Ruschin[2]
[1]*Department of Chemistry, University of Cambridge,*
[2]*Department of Physical Electronics, Faculty of Engineering, Tel-Aviv University,*
[1]*United Kingdom*
[2]*Israel*

1. Introduction

The area of chemical sensors is one of the fastest growing both in research and in commercial fields. Most of the research work in this area is concentrated towards reducing the size of sensors and the identification and quantification of multiple species. Quick response, minimum hardware requirement, good reversibility, sensitivity, and selectivity are expected from an excellent sensor, and hence there is a need for further research. The applications of chemical sensors include quality and process control, biomedical analysis, medical diagnostics, environmental pollution control, continuous and long term monitoring of pollutants and hazardous substances. There are however several outstanding problems hindering applications of chemical sensors based on optical readout. It is widely accepted that in many instances the sensitivity is not the limitation of the sensor. Indeed many sensors display over-sensitivity at the expense of specificity and are vulnerable to noise. In real applications the environment in which sensors are located is not sterile: additional substances present will cause spurious readouts, and moreover, the substances may react over the sensor's surface and readouts will be then cross-correlated.

Methods to overcome these hindrances are addressed in this chapter using porous silicon as a testbed. They are based on signal or statistical analyses of the data acquired and take advantage of the possibility of multi-sensing with properly modified sensor arrays. Several new configurations for optical multi-sensing are presented in this chapter, and demonstrated for ammonia detection. The methods are however generic for optical remote sensing of multiple gas components and can be applied to industrial and environmental gas supervision as well as biomedical applications. The detection of ammonia is based on chemical reaction between ammonia-sensitive dye and the detected molecules. These reactions are accompanied by changes in optical absorption spectrum within the VIS-NIR range. pH sensitive dyes have been widely used for ammonia detection (Malins et al., 1999; Malins et al., 1998; Potyrailo et al., 1994). For these sensors, the response to ammonia vapour is highly dependent upon the level of humidity in the environment since the acid–base reaction of the dye materials is always mediated by water, and therefore calibrating for atmospheric humidity is required for determining true values of ammonia concentration.

2. Porous slicon

Porous silicon (PSi) is typically produced by electrochemical etching of bulk crystalline silicon. The porosity of the produced material is directly proportional to the applied current density during the etching process, providing therefore a simple means to control its refractive index (Vial and Derrien, **1995**). Various optical components such as Bragg and rugate reflectors have been successfully fabricated with porous silicon (Lorenzo et al., 2005). PSi can be used as smart transducer material in sensing applications, and in particular in the detection of vapours (De Stefano et al., 2004a). Upon exposure to chemical substances, several physical quantities, such as refractive index, photoluminescence, and electrical conductivity change drastically. A key feature of a physical transducer, being sensitive to chemical molecules, either in vapour and liquid state, is a high surface area to volume ratio. Moreover, PSi is an available, low cost material, compatible with standard microelectronics processes, so that it can be successfully employed in the realization of smart sensors and microsystems.

2.1 Fabrication

The two main characteristics of porous silicon are the thickness of the porous layer and its refractive index distribution, which depend on electrochemical anodization time and the current density (Pavesi and Mulloni, 1998). Anodization of porous silicon is usually performed at constant or controlled current density. The Si wafer acts as the anode, a platinum spiral wire as the cathode and the electrolyte is composed of an HF solution. The current density applied during the formation process determines the porosity of the porous silicon layer. Generally, higher current density will produce higher porosity, resulting in lower refractive index. Porosity is defined as the fraction of void within the volume of the porous silicon layer. Pore diameters that can be obtained are in the range of 30 Å to 1 μm and porosities are between 10 and 90% (Searson and Macaulay, 1992). It is acceptable to divide the porous silicon into three categories based on the size of its pores; macroporous (for pore diameters larger than 50 nm), mesoporous (for pore diameters between 2 and 50 nm) and microporous (for pore diameters less than 2 nm). The morphology of the pores is affected by several factors such as crystallographic orientation of the Si wafer, doping, resistivity and current density.

Aging, i.e., the slow spontaneous oxidation of PSi, poses a big disadvantage for practical application of porous silicon as sensor. Due to the aging effect, the structural and optical properties of PSi show continuous change with the storage time. One of the common methods to passivate the PSi structures is thermal oxidation, which results in an increase of the hydrophilicity (wetting) ability due to the formation of polar silicon dioxide (SiO_2). The refractive index is also affected by oxidation, it decreases after the oxidation. If PSi is fully oxidized then its refractive index value is between that of air and that of silica.

2.2 Optical properties - reflectance

A porous medium will exhibit optical properties different than those of the same material in bulk. If the typical feature sizes (e.g. pore size) are much smaller than the wavelengths of the incident electromagnetic field, the field in the porous medium encounters an effective dielectric function. Therefore the reflection from PSi layer displays basically a Fabry–Pérot

interference spectrum. The Fabry–Pérot interference phenomenon for thin film is depicted in Fig. 1a; light travelling from one medium encounters a thin film with refractive index n_{eff} and thickness d. Thin film interference involves interference between light reflected from the top interface (air-PSi) of the film and light reflected from the bottom interface (PSi-Si) of the film. Typical interference fringes measured from PSi thin film are illustrated in Fig. 1b. The Fourier transform of the optical reflectivity spectrum provides a simple means to monitor the optical thickness ($n_{eff}d$) of the porous silicon layer (Anglin et al., 2004; Pacholski et al., 2005b). An example is presented in inset of Fig. 1b, where Fourier transform spectrum of the PSi film produces a peak whose position is dependent the optical thickness of the porous layer.

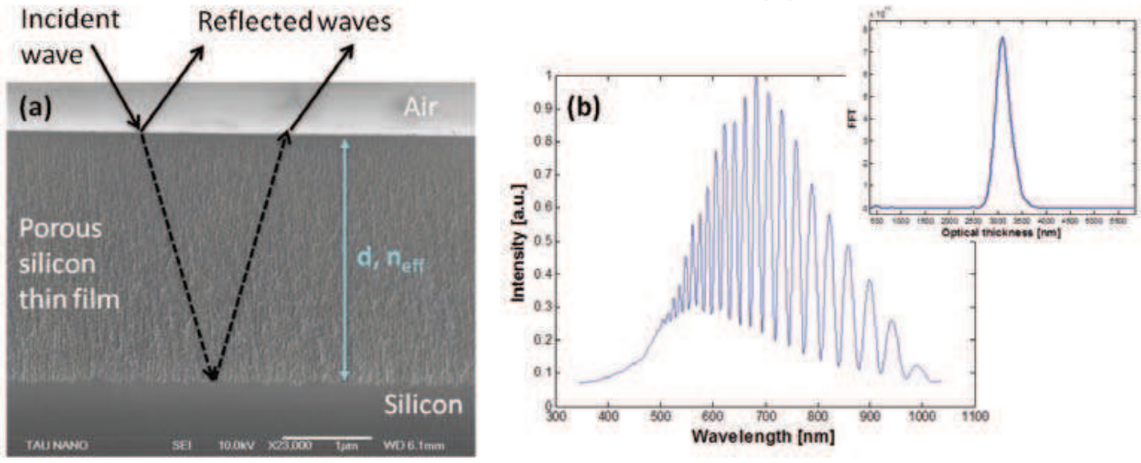

Fig. 1. (a) SEM image of porous silicon cross section. Arrows show light beam reflection from the thin-film with thickness d and refractive index n_{eff}. (b) Reflection spectrum of porous silicon thin-film showing Fabry-Perot interference phenomenon. Inset displays corresponding Fourier transform, where the position of the peak is proportional to the optical thickness.

The refractive index of PSi layer can be determined as a function of the porosity and the wavelength through reflectance measurements. Reflectivity maxima are located at wavelengths determined by the Fabry–Pérot relationship (Eq. 1), where m is the spectral order of the fringe at wavelength λ, θ is the angle, n_{eff} the refractive index of the film and d is the film thickness. The position of the interference maxima for two consecutive maxima, m and m+1 satisfies:

$$2n_{eff}d\cos\theta\cdot\left(\frac{1}{\lambda_m}-\frac{1}{\lambda_{m+1}}\right)=1 \tag{1}$$

If the thickness of the layer is known independently, then the refractive index can be obtained. It is expected that the refractive index of PSi layer should be lower than of bulk Si and higher than air. PSi is a mixture of the substrate silicon and air, therefore the refractive index decreases with increased porosity. The Bruggemann Effective Medium Approximation (Khardani et al., 2007) (Eq. 2) can be successfully applied in order to find the effective index of porous film.

$$(1-p)\frac{\varepsilon_{Si}-\varepsilon_{eff}}{\varepsilon_{Si}+2\varepsilon_{eff}}+p\frac{\varepsilon_{air}-\varepsilon_{eff}}{\varepsilon_{air}+2\varepsilon_{eff}}=0 \quad (2)$$

where p is the film porosity which describes the volumetric fraction of embedding medium (air), ε_{Si} and ε_{air} are the dielectric functions of silicon and the embedding medium, and ε_{eff} is the effective dielectric function for PSi.

The effective dielectric constant of the PSi film undergoes a significant change when vapours enter the pores and replace the air. This effect of capillary condensation occurs in pores with radii below the Kelvin radius, which is given by:

$$r_K=-\frac{2M\gamma\cos\theta}{\rho N_A kT\ln(\frac{P}{P_0})} \quad (3)$$

where N_A is the Avogadro constant, k is the Boltzmann constant, T is the absolute temperature, M is the molecular weight, ρ is the liquid density, r is the radius of the capillary, θ is the contact angle, γ is the surface tension, P_0 is saturation pressure and P is the equilibrium vapour pressure.

When porous silicon is exposed to analytes in the gas phase, capillary condensation causes an increase of its effective refractive index n_{eff}, because air (n=1) is replaced by the condensed analyte vapour (n>1). The increase in the n_{eff} causes red-shift of the maxima of the fringes. Water vapour readily diffuses to the inner regions of the pore structure and adsorbs on the (oxidized) silicon skeleton. Several humidity sensors based on this principle have been proposed in the literature, some designed to detect humidity through changes of the capacitance (Das et al., 2003), or through changes in optical properties of PSi (Oton et al., 2003). Optical changes of PSi have been also used to detect organic vapours by measuring the optical peak-shifts after exposure to vapours of several liquid mixtures. It was possible to detect the presence of chemical substances (Anderson et al., 2003; De Stefano et al., 2004c; Gao et al., 2000; Snow et al., 1999) and also quantitatively characterize binary mixture composition (De Stefano et al., 2004b; Letant and Sailor, 2001).

3. Increasing reliability in porous silicon optical sensors

Reliable detection of chemical and biological materials depends on the selectivity and sensitivity of the system. Although both properties are desirable in any sensing scheme, they often contradict each other. In general, a trade-off exists between probability of true detection and probability of misdetection (Khodarev et al., 2003). Prioritizing these properties is a matter of the specific implementation conditions. Most attempts to produce sensors able of multi-analyte detection usually result in complicated systems that are not totally immune to interfering substances. As a result, new methods that are capable of multi-sensing are required, while maintaining the simple measurement setup and the sensor's cheap price and easy fabrication.

For a single sensor, selectivity is achieved though specific receptor that selectively binds the analyte of interest, i.e. "lock-and-key" design. In order to be able to detect selectively different analytes, the surface of PSi can be functionalized chemically using surface treatments such as oxidation or carbonization (Salonen et al., 2002), or by attaching chemical

or biological receptors (Lugo et al., 2007; Ocampo et al., 2011). In sensor array configurations, the binding elements do not necessarily need to be highly selective to any particular analyte, and the discrimination is achieved using the collective output with signal processing, thus a specific pattern is generated for each analyte. Such patterns may also be obtained from equilibrium or kinetic responses, with the latter often providing additional discrimination and increased sensitivity (Mescheder et al., 2007). The number of sensors in an array has a direct effect on the quality of the discrimination by improving the signal-to-noise ratio, and helps to avoid ambiguity in interpreting the signals if background gases are changing in concentration. Good reviews about chemical cross-reactive sensor arrays can be found in the literature (Albert et al., 2000; Anzenbacher et al., 2010).

After a short overview of different means to increase the reliability PSi sensors, this section is divided to three main sub-sections. Different configurations for multi-sensing using PSi with emphasis on the reliability improvement are presented in each one. Such methods are not limited to porous silicon sensors and can similarly be implemented to other types of sensors.

The work of Islam *et. al.* presents an example for improving selectivity of porous silicon sensor. They demonstrate discrimination of organic vapours using an array of porous silicon sensors having different porosity and pore morphology (Islam et al., 2006). Sensitivity of PSi sensors for different vapours varies significantly with the variations of pore dimensions, and thus facilitates discrimination through the analysis of the array's collective output. The sensitivity of the PSi depends on the physical parameters of the vapours, e.g. surface tension, molecular weight, dimensions, vapour pressure and dipole moment. In this work, the output was analyzed using neural network based pattern recognition for organic vapours, and showed unique fingerprint for each vapour in a mixture. The recognition can be further enhanced either by increasing the number of sensors in the array or by using the data of the response and the recovery time, which are unique for each vapour. Recently, a technique to produce porous silicon samples with gradually varying porosity was reported (Park et al., 2010). It is based on inserting a Si wafer gradually (or by stages) into a HF solution during the anodization process to produce pore-size and layer thickness gradient or various multilayers, on a single substrate. Such lateral pore gradient distribution can also be used as size-exclusion matrix, and is expected to open up application areas involving optical electronic nose systems.

In another example of improving the selectivity, the changes in reflectivity and PL spectra of PSi chips were recorded during the injection of the analyte (Létant et al., 2000). A series of solvent vapours, ethyl esters, and perfumes were investigated and discrimination obtained with PSi sensors was been found to be as good as those obtained with commercial chemiresistive metal oxide sensors. In a similar example, three independent quantities of PSi were measured: the electrical conductance, the photoluminescence intensity, and the wavelength of the optical resonance for different vapours (Baratto et al., 2002). It was shown that it is possible to distinguish between a pollutant like NO_2 and interfering gases like humidity and ethanol by coupling the measurement of optical and electrical quantities. In another example, a gas sensor with two PSi chips that have different hygroscopic properties was used (Jalkanen et al., 2010). Here, the optical and electrical signals were monitored simultaneously, and both sensor types were able to differentiate between the tested analytes.

3.1 Multivariable data based methods

Multivariable data analysis is used to obtain statistical information for a large number of parameters or measurements; it enables identification of the dominant patterns in the data, such as groups and trends. A common method is principal components analysis (PCA), which results in the objects being described by the principal components rather than by the original variables in the data table. PCA is a linear technique that is used to extract the useful information and the relationship between objects and variables, and reveal groupings among sets of cases. It identifies the orthogonal directions of maximum variance in the original data, in decreasing order, and projects the data into lower dimensional space formed by a subset of the highest-variance components. Usually the number of relevant principal components is much less than the number of variables, and a substantial reduction of the number of dimensions can be achieved. In the case of two or three relevant principal components it is possible to represent the data in 2D and 3D plots in which the axes represent the principal components. PCA is a widely used technique in sensor arrays and in 'electronic noses' (Marquis and Vetelino, 2001; Santonico et al., 2008; Uttiya et al., 2008) for evaluation of the array response.

In this section we demonstrate this method for a single porous silicon sensor coated with a sensitive dye for the determination of ammonia concentration in varying humidity. The sensitivity and the response of the sensor to ammonia are strongly affected by the humidity levels, and therefore it is very important to monitor both simultaneously. When the PSi chip is sensitized by pH sensitive dye, humidity induces a red-shift of the fringes (Fig. 2a) and ammonia induces absorption at wavelengths between 500 and 650 nm in the reflected spectrum (Fig. 2b) (also the absorption sensitivity to ammonia is increased by the presence of humidity). Consequently, the reflected spectrum for certain ammonia concentration is different at different relative humidity levels. By monitoring changes in the whole spectrum, we attempt to achieve differentiation using PCA. The results for ammonia gas at 0, 25 and 50% relative humidity (RH) are presented in Fig. 3. This PCA calibration plot shows clear separation of the ammonia measurements at different humidity levels. It might be possible to increase the selectivity if one also monitors the time-dependent curves, as response and recovery, in addition to the equilibrium condition.

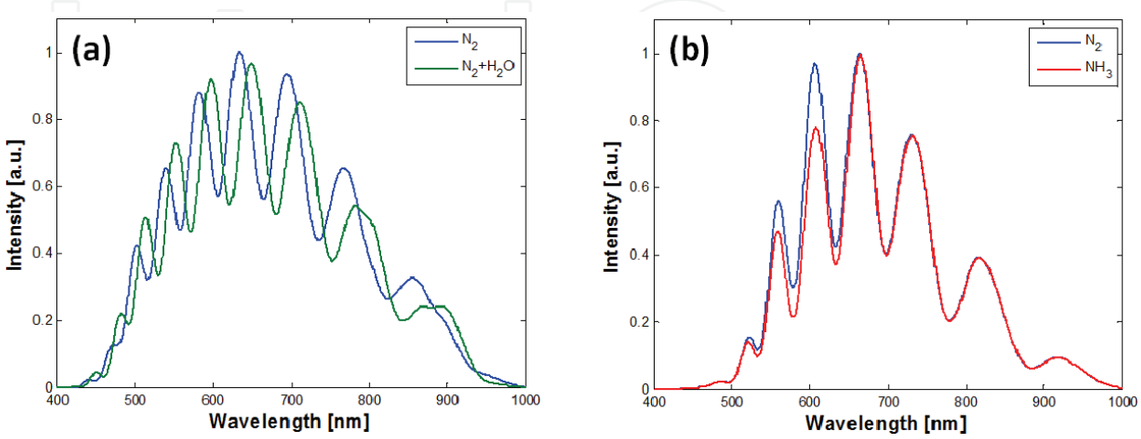

Fig. 2. The effect of (a) humidity and (b) ammonia on the reflection spectrum of PSi sample immobilized with pH dye.

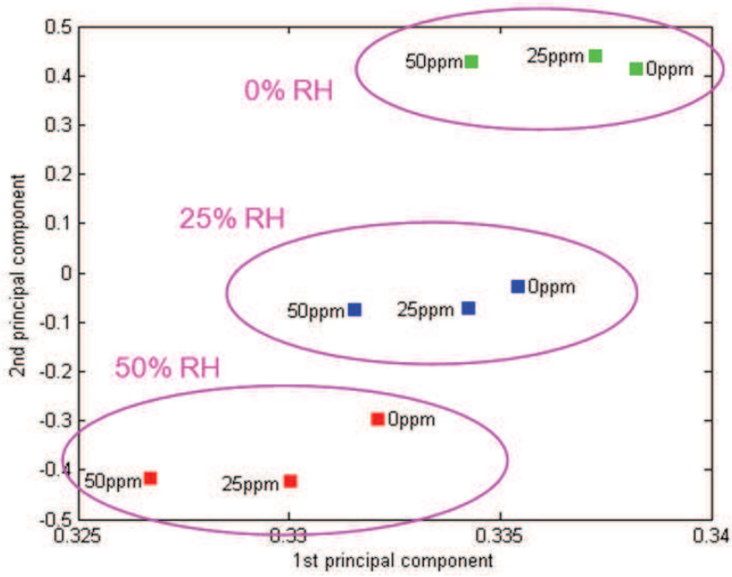

Fig. 3. Calibration plot for ammonia at different humidity conditions, each marked group refers to certain humidity level.

3.2 Muli-sensing via optical multiplexing

In this section we describe an optical non-imaging method for multi-sensing using thin film interference and a single light source and detector (Hutter and Ruschin, 2010). Porous silicon can be successfully employed as a transducer, however any other materials which induce similar spectral interference changes may be used. The method presented here is generic for optical remote sensing of multiple gas components. The device arrangement consists of sectioned porous silicon sensors where each component is sensitive to a different substance. In addition, the different sections can differ in film thickness or refractive index. The combined device is illuminated with a single white-light beam in a non-imaging and distance-independent configuration. The combined reflection is monitored, and the sectioned sensors are designed to provide frequency-encoded patterns which are processed using a fast Fourier transform (FFT) algorithm, allowing real-time monitoring of the effect of several gases by means of single light beam. Fourier transform spectroscopy in PSi samples was reported by M.J. Sailor *et. al.* (Pacholski et al., 2005a; Pacholski et al., 2006) who describe self-compensating interferometric biosensor composed of two layers with different pore diameters for separate sensing of biomolecules. Light reflection from such sensor displays a complex interference spectrum from layers stacked one on top of the other, whose components were resolved by means of Fourier transform. Same setup has been used to detect organic vapours and humidity, thus compensate for fluctuations in humidity (Ruminski et al., 2008).

In an alternative way, the different porous silicon sections are placed one beside the other, on one plane. This arrangement allows the exposure of each section to the same chemical environment and avoids possible partial blocking of stacked films. Each section in the array is made of porous silicon with a different functionality, like a different surface modification or immobilized indicator dye. This arrangement is scalable, with the possibility of increasing

the number of porous silicon sections. In each sample, the PSi film differs either in thickness or porosity, therefore the thin-film reflection spectrum of each of the array components varies in periodicity. This periodicity distinction enables to encode the spectrum in such a way that the distinct variations can be straightforwardly analyzed using spectral data analysis methods such as FFT. The schematic representation of such device arrangement is illustrated in Fig. 4. White light is collimated to illuminate the entire sample and then reflected back from all the sensors simultaneously. Light is collected by a lens and focused into a single reading fibre which feeds the light into a spectrometer. Since no imaging is implemented in the light collection, the obtained spectrum consists of many overlapping interference patterns each reflected from a different sensor section. The non-imaging arrangement is especially attractive for remote sensing or cases where several sensing units are monitored with a common optical source and detector. In order to separate the information regarding each of them, an FFT algorithm is applied on the combined spectrum as seen in Fig. 5. It is desirable that peaks in the Fourier-transformed spectrum for each porous silicon sensor will be well separated along the Fourier co-ordinate, to allow good discrimination. The location of the peak depends on the refractive index (porosity) and the thickness of the layers, and these parameters are easily controlled in the electro-chemical processing of porous silicon.

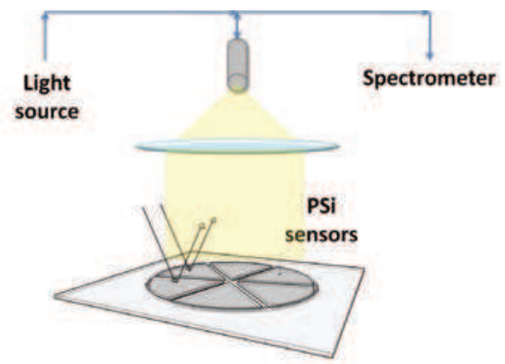

Fig. 4. Schematic presentation of a multi-sensor device based on PSi thin films. Each section is designed to have a specific purpose in the sensing mechanism.

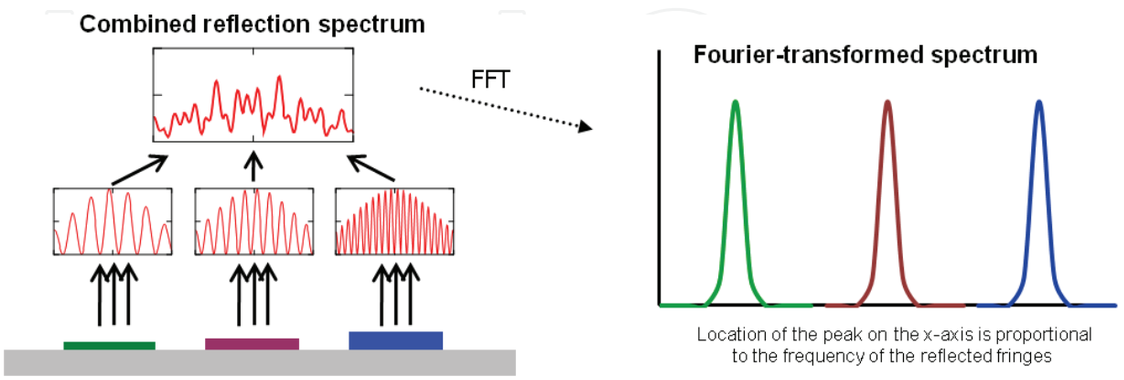

Fig. 5. Illustration of a spectral encoding principle. Each thin film is designed to have a specific reflection spectrum. The combined reflection spectrum is measured and FFT algorithm is then applied. The Fourier-transformed spectrum showing peaks, whose location corresponds to the reflected frequency of each thin film.

It should be noted, that more than one peak is induced in the Fourier domain by a single thin-film (overtones). Avoiding overtone overlap should be taken into account when designing the chip.

Implementation example:

A simple demonstration of such device was fabricated by us, in which the sample was sectioned into two parts: one for water vapour and one for ammonia. Correspondingly, one half was made of oxidized porous silicon and the other one was made of oxidized porous silicon with a chemical pH indicator dye immobilized inside the pores. As discussed earlier, the oxidized half is highly sensitive and reversible towards water vapour, and therefore used as a humidity sensor. The pH indicator dye which was immobilized into the second half, responds to both ammonia concentration and humidity. The independent determination of water vapour concentration is therefore necessary, and by this method this is achieved by a single measurement. The combined use of both sensors enables the separate determination of these two components. The sensor is interrogated with a single white-light beam, and changes in the reflectivity sensor are monitored. The combined interference pattern from both PSi sections is observed and measured under various concentrations of ammonia and water vapour. The structure is designed to frequency encode the reflectivity spectrum and Fourier-transform data-analysis is applied in order to enable simple discrimination between different ammonia and water vapour concentrations. Illustration of the method steps is shown in Fig. 6. The measurements, calibration and analysis of data were performed according to the following sequence: as a first step for each set of measurements, the reflected reference spectrum (measured in dry nitrogen only) was subtracted from all the measured spectra. In the next step, the x-coordinate of reflected spectra was inverted from wavelength (nm) to wavenumbers (nm^{-1}) and a linear interpolation was applied in order to obtain an evenly spaced data set in the inverted new x-axis. Finally a FFT algorithm was applied. Each porous silicon section produces a characteristic peak in the Fourier domain. The position of the peak depends on the porous layer properties, and therefore is unique for each set of fringes. In our case we applied FFT on the difference spectra, i.e. spectrum when exposed to vapour minus the reference spectrum at dry nitrogen.

A schematic illustration of the peaks in Fourier domain due to humidity and dry ammonia is shown in Fig. 6c. When water vapour is introduced into the system, a red-shift of the fringes for both PSi sensors causes peaks to occur in the normalized spectrum and in the Fourier domain at the original periodicity value. The more water vapour infiltrates the pores, the bigger the red shift, the bigger the amplitude of the normalized spectrum and therefore the higher the peak. When dry ammonia is introduced, there is absorbance at 550-650 nm, and the total area of the graph spectrum is reduced. As a consequence, an additional peak at low (DC) frequencies (0-1 nm in the Fourier spectrum) occurs. The magnitude of this peak is therefore sensitive to the ammonia concentration. The oxidized PSi sensor without the pH sensitive dye, shows no response to dry ammonia, and therefore its corresponding peak is absent from the Fourier domain. For a certain ammonia concentration, the reason of the increase of the DC peak with humidity is that the sensitivity of the dye to ammonia is affected by the presence of water vapour.

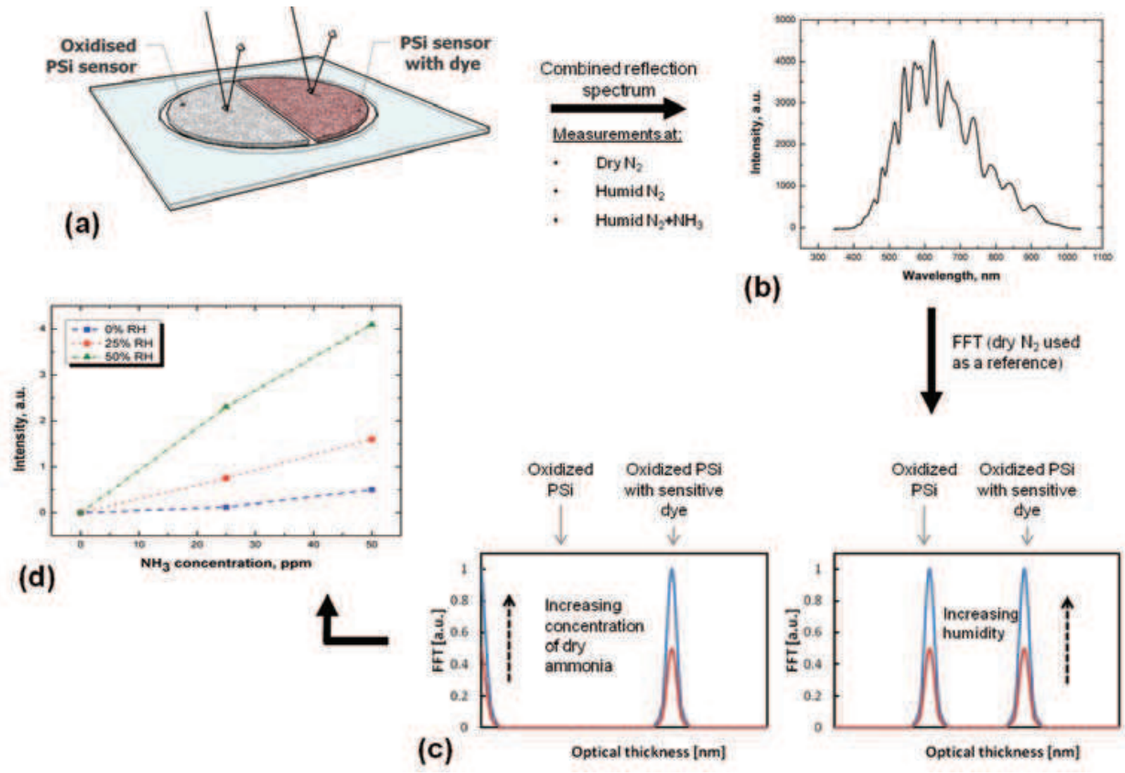

Fig. 6. Illustration of the presented method for ammonia measurement in changing humidity environment. (a) Two PSi sections with different functionality. (b) Measured combined spectrum from two PSi sections, showing interference arising from two thin-films. (c) Schematic illustration of Fourier domain of the two sections once exposed to dry ammonia (left) and once to humidity with no ammonia (right). (d) Experimental result demonstrating the ability of the method to determine ammonia at different relative humidity (RH) values.

In this section a device consisting of sectioned porous silicon, able of simultaneous sensing of different chemical substances in gaseous phase was presented. Each section differs from the other in one or more of its fabrication parameters, namely: thickness, porosity or chemical sensitization. The method was applied to the determination of ammonia in a humid environment, by simultaneous monitoring of two PSi sensors with single light beam. In a broader context, the device provides an *in-situ* method of chemical analysis by gathering information about changes in both the absorption and refractive index in a chemical reaction. Here it is possible to compensate for illumination fluctuations by placing an additional inert PSi thin film. A drawback of this method is that device calibration is required for the determination of the ammonia concentration in changing humidity environment.

3.3 Sensor arrays based on indicator gradient

In this section, we present another method for improving the detection reliability for a given chemical in the presence of other chemical agents or perturbations that generate spurious signals (Hutter et al., 2011). The method provides a thresholding parameter which can be tuned by the user according to his priority considerations between sensitivity and

selectivity. We demonstrate the method using a dye immobilised porous silicon optical detector array aimed at identifying ammonia gas at varying humidity conditions and unstable illumination.

In general, a chemical or biological sensor uses a probe (or receptor) to react with the analyte of interest, leading to a measurable signal. The signals' reliability may depend on the number of probes available to react with the analyte, while the precise type of such dependency differs between different sensor types and working conditions. In the method presented here, the available probes are chosen in a manner such that sensors are of the same type but generate a signal varying sensitivity, approximately linear with respect to the probe concentration on their surface. As will be shown in the following, the resulting signal vector accommodates for sensitivity and selectivity towards the analyte, and does not require training or calibration for its detection. We note that the linearity assumption is not strict but will limit the method for analyte concentrations that either saturate completely the sensor or are below its minimum detectable limit. A schematic drawing of such a sensor array is depicted in Fig. 7. The demonstrated array is comprised of n optical sensors that are similar in all physical parameters other than the probe concentration. A common light source is applied to all sensors, and the reflected light from each sensor is measured at a single wavelength by a dedicated detector. The detector array output is a vector of signals s. The vector of output signals s is correlated with the probe concentration gradient p. The system's direct internal light source I_{dir} is used for all sensors, where the detector array is exposed to additional undetermined external light I_{ext}. The output of the correlator y compared to a threshold θ; when it is exceeded, the analyte presence, is inferred.

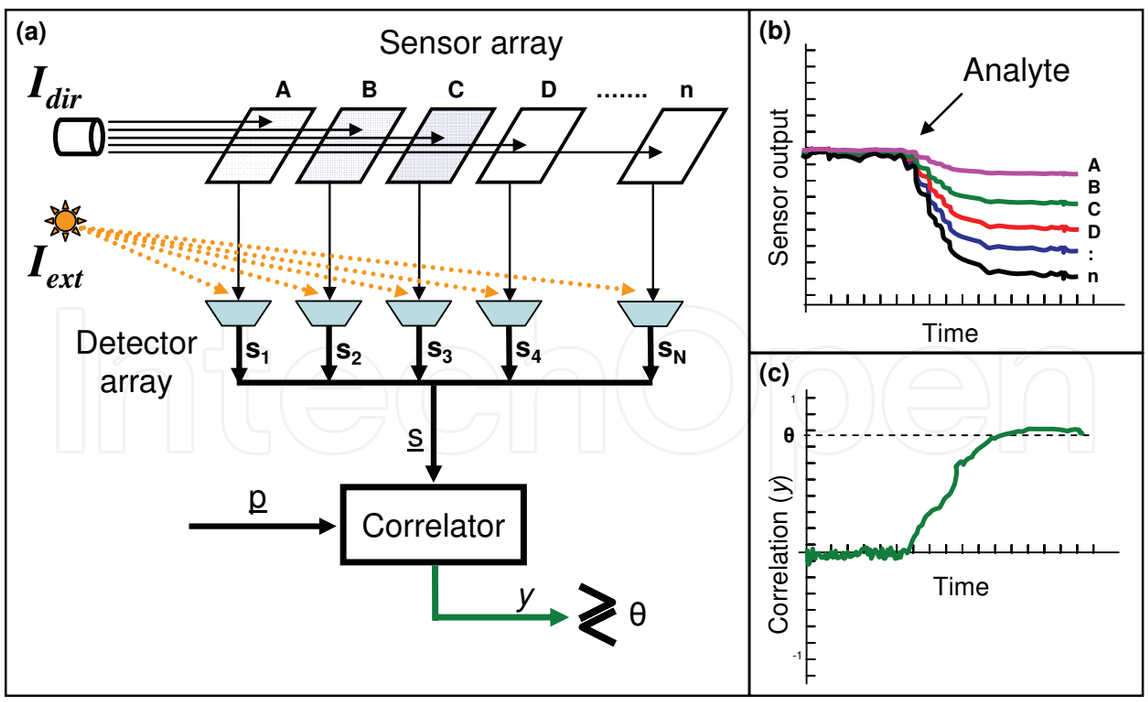

Fig. 7. (a) Sensor array detector illuminated with a light source for the optical readout, and also subjected to some external illumination. (b) Output signal of each sensor. (c) Output of the correlator.

The offset of each sensor is canceled by using the baseline steady state signal as a reference (e.g., averaging s_i over time after initialization, when there is no analyte in the system). We therefore assume for simplicity that the sensitivity vector $\underline{h}$ is given by the product of the probe concentration vector $\underline{p}$ with some unknown transduction factor T:

$$\underline{h} = \mathrm{T} \cdot \underline{p} \tag{5}$$

The array output $\underline{s}$ is:

$$\underline{s} = I_{dir} \cdot \underline{h} \cdot x + \underline{v} \tag{6}$$

where x is the analyte concentration, and $\underline{v}$ vector of the sum of external light source intensity fluctuations at the detector (denoted I_{ext}) and other time dependent noises. We note that T may incorporate many different effects such as aging or the presence of other chemicals that may enhance or degrade the sensor's signal. Since in most cases both T and x are unknown, and coupled in the common case of a single sensor, their efficient estimation cannot be achieved without a thorough calibration process of the factor T which in many cases depends on a series of environmental conditions. We emphasize that the method developed here does not require the a-priori knowledge of T, while preserving the ability to infer the presence or absence of the analyte, which is sufficient in many practical situations.

The detection algorithm should provide a decision, based on the sensor array output, regarding whether the analyte is present or not. As we are unable to estimate a priori the concentration of the analyte, we provide a metric for the array output fit to the expected behavior when the analyte is present. This metric will be compared to a threshold, which can be set per user specification. When the metric exceeds this threshold, a signal indicating the presence of the analyte will be asserted. Lowering this threshold will raise the probability of false alarms, therefore decreasing the specificity of the system while improving its sensitivity, whereas raising it will lower the probability of misdetection, at the cost of lower sensitivity. For the system modeled here, we used the normalized correlation coefficient (NCC) as the metric (Pratt, 2001). In this approach the output vector of the sensor array $\underline{s}$ is correlated with the sensors probe quantity gradient vector $\underline{p}$ and normalized with the norm of both vectors:

$$y = \begin{cases} \dfrac{\sum_{i=1}^{n}\left(s_i - \bar{s}\right)\left(p_i - \bar{p}\right)}{\sqrt{\sum_{i=1}^{n}\left(s_i - \bar{s}\right)^2 \sum_{i=1}^{n}\left(p_i - \bar{p}\right)^2}} & \sum_{i=1}^{n}\left(s_i - \bar{s}\right)^2 \neq 0 \\ 0 & \sum_{i=1}^{n}\left(s_i - \bar{s}\right)^2 = 0 \end{cases} \tag{7}$$

With

$$\bar{s} = \frac{1}{n}\sum_{i=1}^{n} s_i \tag{8}$$

And

$$\bar{p} = \frac{1}{n}\sum_{i=1}^{n} p_i \tag{9}$$

y assumes values between 1 and -1, and it can be determined in real time. As the analyte is introduced into the system, its value increases.

Regarding the immunity to light source fluctuations and transduction changes, in the calculation of y, we subtract the mean of signal vector $\underline{s}$. When the detectors of the array are exposed to I_{ext}, e.g. to environmental lighting, a uniform additive signal is expected for all elements of $\underline{s}$. The NCC should be invariant with this addition. Fluctuations in I_{dir} or T may also create noisy output which is not compensated by the subtraction of average. However, since all sensor outputs are scaled by I_{dir} and T as in Eq. 6, normalizing by the norm of $\underline{s}$ makes y independent of these factors, therefore independent of their changes over time, as long as the changes do not take place within a single measurement event, taken from all detectors.

Implementation example:

The method was implemented in a PSi ammonia gas detector, using bromocresol purple, which is a pH sensitive dye. The array is composed of four oxidzed porous silicon sensors, each coated with a different concentration of the dye (sensor A coated with the lowest amount, and sensor D with the highest amount). The resulting signal vector is collected by measuring the absorption at a single wavelength at each sensor. Ammonia gas induces absorption at 500 - 650 nm in the reflected spectrum, in our study we have chosen a wavelength of 557 nm. As stated, each sensor was coated with different amounts of the sensitive dye. Threrefore, the magnitude of the signal should be proportional to the quantity of the coated dye, i.e. the sensitivity of the sensor increases as the quantity of the sensitive dye increases (Fig. 8a). When humidity is present, water vapors condense inside the pores via capillary condensation causing an increase in the refractive index of the porous layer. This increase in optical thickness causes a red-shift in the fringes of the reflected light from the sensor. According to that effect, the signal should not be proportional to the quantity of the coated dye (Fig. 8b). On the other hand, in case of ammonia in humid environment (Fig. 8c), the increase in the output signal is still expected to increase with the qunatity of dye. According to the graph of Fig. 8b, the signal generated from sensor D is lower than expected; this performance degradation may be due to defective coating or saturation. We deliberately did not omit this sensor's output from the subsequent analysis, to show the robustness of the method against failure of a single sensor in the array.

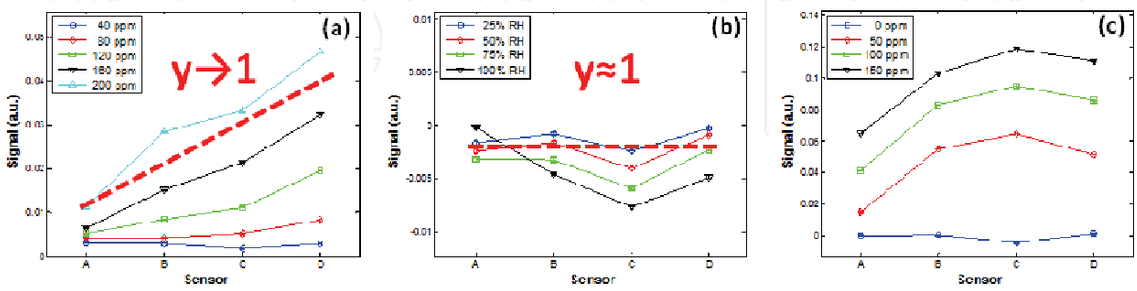

Fig. 8. Signal generated from four sensors at a presence of (a) different ammonia concentrations (b) different humidity conditions, and (c) ammonia at 25% RH.

Fig. 9a shows the value of the correlator parameter y vs. ammonia concentrations in dry air and in the presence of 25% RH (relative humidity). Fig. 8 shows the probability density

function of y, showing a good separation. The choice of threshold value of the NCC will vary according to the measurement scenario and practical considerations. Setting the threshold for detection between 0.6 and 0.65 will ensure the positive detection of ammonia with negligible chance of false detection due to pure humidity. The value of *y* for humid ammonia at high concentrations is lower than that of dry ammonia in spite of the fact that the sensitivity is lower for the dry case. This is probably due to sensor *D* which generated lower signals than expected (see Fig. 8c). We note that even in this case the system retains its reliability.

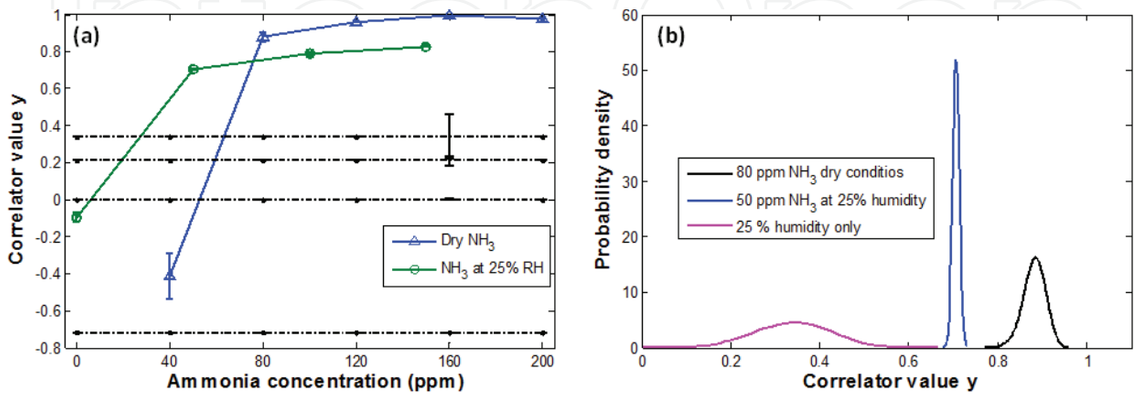

Fig. 9. (a) The NCC for dry ammonia and ammonia at 25 % RH. The horizontal lines correspond to the correlation coefficient at 25, 50, 75 and 100% RH. (b) The probability plot as a function of correlation coefficient.

One of the main features of the method proposed here is improved selectivity. We note that this feature comes at the expense of sensitivity and accurate estimation of the analyte concentration. The sensitivity of a single sensor to changes in concentration levels was found to be below 1 ppm. We trade this superior property with the discrimination ability, as the high sensitivity in any single sensor does not facilitate discriminative ability at a single wavelength. Using the data from each of the sensors, the overall sensitivity is degraded. Using the gradient array, we gain immunity to humidity generated signals; with the normalization, we gain immunity to light source fluctuations. Another advantage of the proposed method is its immunity to tolerable fluctuations in the transduction factor T.

To summarise this section:

- The gradient method is aimed at identifying ammonia gas at a single wavelength at varying humidity, unstable illumination and other disruptive effects. This feature suggests the possibility of using a laser source to monitor the sensor, with clear benefits in signal magnitude and range.
- It is best suited to function as an alarm generator working in a yes/no mode for the presence of a given hazardous substance.
- Simple correlation of the signal vector with an expected gradient-like response enables detection of ammonia (linearity assumption).
- No calibration or training is required.
- It improves immunity to false signals created by changes in illumination intensity and the humidity of the environment.
- Trade off – increased selectivity, decreased sensitivity.

- Optimization may be achieved by increasing the number of sensors, optimizing dye quantities, using a more selective dye to ammonia or changing the working wavelength.

The method of detection is generic and applicable to further types of sensor arrays where the probe concentration can be controlled.

4. Conclusion

In this chapter several optical methods for improving the reliability and specificity of the detection of one or more chemical in the presence of other chemical agents that generate spurious signals were presented. Optical properties of nano-structured porous silicon were employed for this purpose. The methods were demonstrated for detection of ammonia in gaseous phase, which is important for industrial or clinical applications.

5. References

Albert, K. J., Lewis, N. S., Schauer, C. L., Sotzing, G. A., Stitzel, S. E., Vaid, T. P. and Walt, D. R. (2000). *Chemical Reviews* 100, 2595-2626.

Anderson, M. A., Tinsley-Bown, A., Allcock, P., Perkins, E. A., Snow, P., Hollings, M., Smith, R. G., Reeves, C., Squirrell, D. J., Nicklin, S. and Cox, T. I. (2003). *Physica Status Solidi a-Applied Research* 197, 528-533.

Anglin, E. J., Schwartz, M. P., Ng, V. P., Perelman, L. A. and Sailor, M. J. (2004). *Langmuir* 20, 11264-11269.

Anzenbacher, J. P., Lubal, P., Bucek, P., Palacios, M. A. and Kozelkova, M. E. (2010). *Chemical Society Reviews* 39, 3954-3979.

Baratto, C., Faglia, G., Sberveglieri, G., Gaburro, Z., Pancheri, L., Oton, C. and Pavesi, L. (2002). *Sensors* 2, 121-126.

Das, J. O., Dey, S., Hossain, S. M., Rittersma, Z. M. C. and Saha, H. (2003). *Ieee Sensors Journal* 3, 414-420.

De Stefano, L., Moretti, L., Lamberti, A., Longo, O., Rocchia, M., Rossi, A. M., Arcari, P. and Rendina, I. (2004a). *Nanotechnology, IEEE Transactions on* 3, 49-54.

De Stefano, L., Moretti, L., Rendina, I. and Rossi, A. M. (2004b). *Physica Status Solidi a-Applied Research* 201, 1011-1016.

De Stefano, L., Rendina, N., Moretti, L., Tundo, S. and Rossi, A. M. (2004c). *Applied Optics* 43, 167-172.

Gao, J., Gao, T. and Sailor, M. J. (2000). *Applied Physics Letters* 77, 901-903.

Hutter, T., Horesh, M. and Ruschin, S. (2011). *Sensors and Actuators B: Chemical* 152, 29-36.

Hutter, T. and Ruschin, S. (2010). *IEEE Sensors Journal* 10, 97-103.

Islam, T., Das, J. and Saha, H. (2006). In "Sensors, 2006. 5th IEEE Conference on", pp. 1085-1088.

Jalkanen, T., Tuura, J., Mäkilä, E. and Salonen, J. (2010). *Sensors and Actuators B: Chemical* 147, 100-104.

Khardani, M., Bouaicha, M. and Bessais, B. (2007). *Physica Status Solidi C - Current Topics in Solid State Physics,* Vol 4 No 6 4, 1986-1990.

Khodarev, N. N., Park, J., Kataoka, Y., Nodzenski, E., Hellman, S., Roizman, B., Weichselbaum, R. R. and Pelizzari, C. A. (2003). *Genomics* 81, 202-209.

Letant, S. E. and Sailor, M. J. (2001). *Advanced Materials* 13, 335-338.
Lorenzo, E., Oton, C. J., Capuj, N. E., Ghulinyan, M., Navarro-Urrios, D., Gaburro, Z. and Pavesi, L. (2005). *Applied Optics* 44, 5415-5421.
Lugo, J. E., Ocampo, M., Kirk, A. G., Plant, D. V. and Fauchet, P. M. (2007). *Journal of New Materials for Electrochemical Systems* 10, 113-116.
Létant, S. E., Content, S., Tan, T. T., Zenhausern, F. and Sailor, M. J. (2000). *Sensors and Actuators B: Chemical* 69, 193-198.
Malins, C., Doyle, A., D. MacCraith, B., Kvasnik, F., Landl, M., Simon, P., Kalvoda, L., Lukas, R., Pufler, K. and Babusik, I. (1999). *Journal of Environmental Monitoring 1*, 417-422.
Malins, C., Landl, M., Simon, P. and MacCraith, B. D. (1998). *Sensors and Actuators B: Chemical* 51, 359-367.
Marquis, B. T. and Vetelino, J. F. (2001). *Sensors and Actuators B: Chemical* 77, 100-110.
Mescheder, U., Bauersfeld, M. L., Kovacs, A., Kritwattanakhron, J., Muller, B., Peter, A., Ament, C., Rademacher, S. and Wollenstein, J. (2007). In "Solid-State Sensors, Actuators and Microsystems Conference, 2007. TRANSDUCERS 2007. International", pp. 1417-1420.
Ocampo, M., Doti, R., Faubert, J. and Lugo, E. (2011). In "Biosensors - Emerging Materials and Applications". InTech, ISBN: 978-953-307-328-6.
Oton, C. J., Pancheri, L., Gaburro, Z., Pavesi, L., Baratto, C., Faglia, G. and Sberveglieri, G. (2003). *Physica Status Solidi a-Applied Research* 197, 523-527.
Pacholski, C., Sartor, M., Sailor, M. J., Cunin, F. and Miskelly, G. M. (2005a). *Journal of the American Chemical Society* 127, 11636-11645.
Pacholski, C., Sartor, M., Sailor, M. J., Cunin, F. d. r. and Miskelly, G. M. (2005b). *Journal of the American Chemical Society* 127, 11636-11645.
Pacholski, C., Yu, C., Miskelly, G. M., Godin, D. and Sailor, M. J. (2006). *Journal of the American Chemical Society* 128, 4250-4252.
Park, S. H., Lee, K. W. and Kim, Y. Y. (2010). *Thin Solid Films* 518, 2860-2863.
Pavesi, L. and Mulloni, V. (1998). *Journal of Luminescence* 80, 43-52.
Potyrailo, R. A., Golubkov, S. P., Borsuk, P. S., Talanchuk, P. M. and Novosselov, E. F. (1994). *Analyst* 119, 443-448.
Pratt, W. K. (2001). "Digital Image Processing".
Ruminski, A. M., Moore, M. M. and Sailor, M. J. (2008). *Advanced Functional Materials* 18, 3418-3426.
Salonen, J., Laine, E. and Niinisto, L. (2002). *Journal of Applied Physics* 91, 456-461.
Santonico, M., Pittia, P., Pennazza, G., Martinelli, E., Bernabei, M., Paolesse, R., D'Amico, A., Compagnone, D. and Di Natale, C. (2008). *Sensors and Actuators B: Chemical* 133, 345-351.
Searson, P. C. and Macaulay, J. M. (1992). *Nanotechnology* 3, 188.
Snow, P. A., Squire, E. K., Russell, P. S. J. and Canham, L. T. (1999). *Journal of Applied Physics* 86, 1781-1784.
Uttiya, S., Pratontep, S., Bhanthumnavin, W., Buntem, R. and Kerdcharoen, T. (2008). In "Nanoelectronics Conference, 2008. INEC 2008. 2nd IEEE International", pp. 618-623.
Vial, J.-C. and Derrien, J. (1995). "Porous Silicon Science and Technology". Springer Verlag, Berlin.

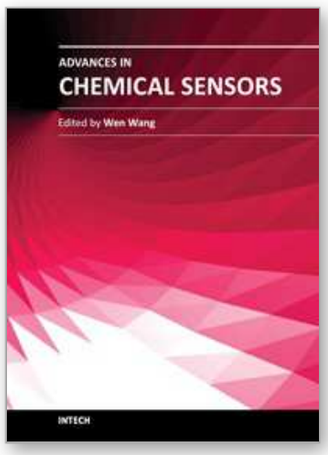

Advances in Chemical Sensors

Edited by Prof. Wen Wang

ISBN 978-953-307-792-5
Hard cover, 358 pages
Publisher InTech
Published online 20, January, 2012
Published in print edition January, 2012

The chemical sensor plays an essential role in the fields of environmental conservation and monitoring, disaster and disease prevention, and industrial analysis. A typical chemical sensor is a device that transforms chemical information in a selective and reversible way, ranging from the concentration of a specific sample component to total composition analysis, into an analytically useful signal. Much research work has been performed to achieve a chemical sensor with such excellent qualities as quick response, low cost, small size, superior sensitivity, good reversibility and selectivity, and excellent detection limit. This book introduces the latest advances on chemical sensors. It consists of 15 chapters composed by the researchers active in the field of chemical sensors, and is divided into 5 sections according to the classification following the principles of signal transducer. This collection of up-to-date information and the latest research progress on chemical sensor will provide valuable references and learning materials for all those working in the field of chemical sensors.

InTech Europe
University Campus STeP Ri
Slavka Krautzeka 83/A
51000 Rijeka, Croatia
Phone: +385 (51) 770 447
Fax: +385 (51) 686 166
www.intechopen.com

InTech China
Unit 405, Office Block, Hotel Equatorial Shanghai
No.65, Yan An Road (West), Shanghai, 200040, China
中国上海市延安西路65号上海国际贵都大饭店办公楼405单元
Phone: +86-21-62489820
Fax: +86-21-62489821

IntechOpen